

Polarization effects in the channel of an organic field-effect transistor

H. Houili, J.D. Picon and L. Zuppiroli*

*Laboratoire d'Optoélectronique des Matériaux Moléculaires, STI-IMX-LOMM, station 3,
Ecole Polytechnique Fédérale de Lausanne, CH-1015, Lausanne, Switzerland.*

M.N. Bussac

*Centre de Physique Théorique, UMR-7644 du Centre National de la Recherche Scientifique,
Ecole Polytechnique, F-91128 Palaiseau Cedex, France.*

Abstract

We present the results of our calculation of the effects of dynamical coupling of a charge-carrier to the electronic polarization and the field-induced lattice displacements at the gate-interface of an organic field-effect transistor (OFET). We find that these interactions reduce the effective bandwidth of the charge-carrier in the quasi-two dimensional channel of a pentacene transistor by a factor of two from its bulk value when the gate is a high-permittivity dielectric such as (Ta_2O_5) while this reduction essentially vanishes using a polymer gate-insulator. These results demonstrate that carrier mass renormalization triggers the dielectric effects on the mobility reported recently in OFETs.

PACS numbers: 72.80.Le, 73.40.Qv, 32.10.Dk, 77.22.Ch

*Corresponding author: libero.zuppiroli@epfl.ch

I. INTRODUCTION

Organic field-effect transistors (OFETs) with high charge-carrier mobilities are essential components for high-speed organic electronic applications. For this reason, it is of crucial importance to unravel the origin of charge transport in these devices. Several experimental studies have shown that the difference in the charge-carrier transport observed in bulk organic semiconductors and within the quasi-two dimensional channel near the gate-insulator interface in OFETs is associated with the effects of disorder and interfacial traps [1, 2, 3, 4]. More intriguing is a growing body of evidence demonstrating the strong influence of the dielectric permittivity of the gate-insulator on the charge-carrier mobility in OFETs [5, 6]. Veres et al. [5] have studied the case of triarylamine polymer transistors in which measured mobilities well below $10^{-2} \text{ cm}^2/\text{V s}$ can be unambiguously attributed to hopping between localized states. On the other hand, Stassen et al. [6] obtained much higher values, from 1 to $20 \text{ cm}^2/\text{V s}$, in single-crystalline rubrene transistors in which conduction is more intrinsic. A surprising finding in both cases is the drastic decrease of the mobilities as the dielectric constant of the gate-insulator is increased systematically using different dielectric materials. Such observation in devices governed by vastly different charge-transport mechanisms strongly suggests an effect due to the interactions of the charge carriers with the gate-dielectric. These interactions can lead to the renormalization of the bare mass of the charge carriers in the conducting channel of OFETs, providing an explanation for the observed dielectric effects on the mobility as reported in Refs. [5, 6].

In this work, we present a theoretical calculation of the renormalized band mass of charge carriers in the conducting channel of OFETs by looking at two important interactions experienced by charges at the interface of an organic semiconductor with a dielectric material. The first one, purely electronic in origin, is the image force due to the polarization discontinuity at the gate-dielectric interface. The second involves the Coulomb interaction of the charge carriers with surface polar phonons of the dielectric. To illustrate the basic concepts of our calculations and their general applicability to any organic semiconductor, we choose pentacene as a model system since its lattice structure, bandwidth, polarizabilities, and Huang-Rys factors are well-known compared with other organic semiconductors. We find that, in pentacene, the cumulative effect of the electronic and surface-lattice polaronic interactions is to reduce the effective bandwidth by a factor of two as the relative static

dielectric constant of the gate materials is varied from 1 to 25. Within the tight-binding model, such a decrease in the transfer integral can be viewed as a concomitant increase in the effective mass by the same factor. We will suggest that such renormalization of the band properties triggers the effects reported in Refs. [5, 6].

II. TIME SCALES

The non-interacting band properties of a perfect pentacene crystal along all crystallographic directions have been calculated by Cheng et al. [7]. For the bare transfer integral, J , between molecules along the direction of easy propagation in the (a, b) -plane, they obtain $J = 100$ meV from which one gets $\hbar/J \simeq 4 \times 10^{-14}$ s as the characteristic time for in-plane Bloch-wave formation. The corresponding transfer time in the perpendicular c -axis direction, \hbar/J_{\perp} , is thirty times longer than in the plane. Thus, in the presence of scattering which substantially reduces the Bloch-wave lifetime, the carrier motion is essentially two-dimensional.

The above considerations allow for the classification of the various interactions experienced by charge carriers in organic semiconductors. For fast interactions with characteristic times shorter than \hbar/J , the charge can be assumed to be located on a single molecular site. In pentacene, this is the situation encountered during the interaction of the carrier with the electronic polarizability of the medium or in intramolecular charge-transfer as well as the coupling with intramolecular carbon stretching vibrations with frequencies around 1360 cm^{-1} . Since fast interactions arise prior to the formation of the Bloch-wave, they have the effect of dressing the charge with a polarization cloud or a lattice deformation cloud. Slow interactions, on the other hand, have characteristic times much longer than \hbar/J . They act directly on the Bloch-wave or the localized state. Such is the case for interaction of the charge carrier with low-energy intermolecular thermal phonons and librations which, in many cases, can be considered as static with respect to the two-dimensional band motion. These interactions scatter the Bloch-wave or localize the electronic states when the disorder they introduce is large enough. The interaction of the charge with the surface polar phonons of the gate insulator occurs in the intermediate time scale regime. An interesting discussion of time scales can also be found in the first chapter of the book by Silinsh and Čápek [8].

Because they dress the charge with a polarization cloud or lattice deformation, fast pro-

cesses lead to a renormalization of the bare transfer integrals J and J_{\perp} and consequently increase the effective mass along all crystal directions. The case involving electron-phonon interactions has been discussed by several authors, including Appel [9] and Davydov [10]. The purely electronic effects were treated by three of us in an earlier work [11] in which we calculated the renormalization effect due to the electronic polarizability in the bulk of the organic semiconductor. In this work, these calculations will be extended to the situation encountered by carriers at the gate-dielectric interface in OFETs. We shall treat both electronic and lattice effects. The Fröhlich surface polaron at the oxide surface was already studied by Kirova and Bussac [12] for an isotropic organic crystal. The entire problem will be revisited here for the two-dimensional layer of the anisotropic crystal. The slow processes involving low-energy phonons, librations and other quasi-static or static sources of scattering and localization will be discussed and treated elsewhere.

We have to emphasize that, because they are faster than 10^{-14} s, the polarization processes studied here involve only the high-frequency dielectric response of the materials constituting the interface and not the usual low frequency (static) permittivity.

For the sake of clarity and to highlight the important aspects of this work, we summarize the major results of our calculations in the next section. The details of these calculations will be given in separate appendices.

III. RESULTS

In rubrene- or acene-based organic field-effect transistors, the interface with the oxide or polymer gate-insulator involves the highly conducting (a, b) -plane of the organic semiconductor. Our calculation of the variation of the effective transfer integral, J_{IV} , for conduction in this plane is shown in Fig.1 as a function of the static dielectric constant of the gate-insulator. In the results of Fig.1, the charge-carrier is assumed to be located on the first monolayer close to the gate-interface. In the case where the charge is on the second monolayer, we find that there is basically no effect of the dielectric on the transfer integral which then takes the bulk value. These results are obtained from the combined effects of four different interactions which have been treated separately according to their time scales from the fastest to the slowest as discussed below.

1. *Electronic polarization* (J^I). The dynamical renormalization of the carrier motion due

to electronic polarization is different in the bulk and at the interface. At an interface, an image field is generated which is attractive when the high-frequency dielectric constant, ϵ_{∞} , of the gate-insulator is greater than that of the organic semiconductor as is the case for oxides, and is repulsive otherwise as in the case of polymers or air-gap insulators. This image field is typically of the same order of magnitude as the applied gate fields to which it is added or subtracted. The magnitude of the image potential under usual experimental conditions is displayed in Fig.2 as a function of the distance z from the interface. At large distances, the classical expression for the image field holds and the image potential is written as,

$$E_p(z) - E_p(\infty) = -\frac{e^2}{16\pi\epsilon_0 z} \left(\frac{\epsilon_{\infty,2} - \epsilon_{\infty,1}}{\epsilon_{\infty,1}(\epsilon_{\infty,2} + \epsilon_{\infty,1})} \right) \quad (1)$$

where $\epsilon_{\infty,1}$ and $\epsilon_{\infty,2}$ are the high-frequency dielectric constants of the semiconductor and the gate-insulator, respectively. However, corrections to this expression associated with lattice effects show up close to the interface.

The increase in the carrier effective mass due to the electronic polarization cloud is slightly different in the bulk or when it crosses the interface. The details of these calculations are given in Appendix A. They lead to a renormalized intermolecular charge-transfer integral $J^I < J$.

2. *Electronic displacement (J^{II})*. The strong dependence of the mobility and the effective mass with the dielectric permittivity of the gate-insulator seen in experiments, as well as large corrections to the bulk electronic polarization energy near the interface shown in Fig.2, suggest that the first two monolayers next to the dielectric interface dominate the charge transport particularly in the presence of a significant gate field [2]. At even higher fields, one may expect that not only is the charge localized on the first monolayer but its electronic wavefunction is squeezed towards the part of the molecule closer to the insulator. This displacement of the charge distribution on the molecule is also a fast process, controlled by the transfer integral $t_{//} \sim 1$ eV within the molecule which is more than an order of magnitude larger than J^I . This fast process decreases further the transfer integral to J^{II} . The recent semi-empirical quantum-chemistry calculation performed by Sancho-García et al. [13] suggests that this effect is completely negligible in pentacene where the charge-carrier distribution remains perfectly centered even at

very high fields (100 MV/cm). In this case $J_{II} = J_I$. The final result of our calculation presented in Fig. 1 was established in the frame of this hypothesis that we consider as the most reliable at the moment. Nevertheless, in Appendix B another approach is presented which shows that much larger effects would be expected if the charge-carrier distribution on the molecule is allowed to be displaced by values of a few angstroms at high gate fields of 10 MV/cm.

3. *Intramolecular vibrations* (J^{III}). Intramolecular vibrations close to 1360 cm^{-1} in pentacene are strongly coupled to the carrier because they change the π -alternation typical of conjugated molecules. Because these atomic motions are faster than the electronic polaron motion defined by the renormalization transfer integral J^{II} , they also contribute to a further reduction of J^{II} by a constant factor of 0.75, independent of the distance from the interface as well as the applied field ($J^{III} \simeq 0.75J^{II}$). Appendix C reviews how this factor is calculated.
4. *Fröhlich polaron at the oxide surface* (J^{IV}). Oxides are polar materials. Thus, the infrared-active phonon modes which modulate the metal-oxide bonds are strongly coupled to charge carriers sitting at their surface. In aluminum oxide, for instance, the most active mode of this kind is situated at 46 meV [14]. This value is of the same order of magnitude as the effective, in-plane, transfer integral renormalized upon corrections due to the above-mentioned interactions.

The construction of a lattice deformation cloud in the oxide is the object of Appendix D. The polarization interaction energy of the charge with this cloud causes further attraction of the charge to the surface and to the subsequent increase of the effective mass. The calculation is performed in the intermediate coupling regime because here the coupling parameter which controls the process, $\alpha_{\text{eff}}(z)$, defined in Appendix D, is of the order of unity in the first monolayer, and of the order of 0.1 in the second one.

The total binding energy of the carrier in the presence of a gate-insulator includes both the electronic and surface polaron effects arising from the electronic image force potential and the lattice deformation potential at the interface associated with the above interactions. Within a tight-binding model, these effects are incorporated into a renormalized effective

transfer integral J_{IV} given by,

$$J_{IV} = J \left(\frac{J^I}{J} \right) \left(\frac{J^{II}}{J^I} \right) \left(\frac{J^{III}}{J^{II}} \right) \left(\frac{J^{IV}}{J^{III}} \right) \quad (2)$$

Table III provides a summary of all these factors in the order of increasing time-scale characterizing each interaction.

IV. CONCLUSION

The experimental results have clearly shown that the mobilities obtained in organic field-effect transistors are much larger in devices built with an air-gap or a polymer gate-insulator [1, 5, 6] than those using high-permittivity oxide gate dielectrics. Our theoretical results discussed above provide some insight into the origin of these effects.

Given that the bandwidth is four times the transfer integral as suggested in the quantum chemistry calculations of Ref. [15] and starting from a value of 390 meV [7], the effective bandwidth becomes 231 meV in bulk pentacene [11]. It is reduced to 155 meV in an OFET with an aluminum oxide gate insulator (Al_2O_3), to 146 meV close to a Ta_2O_5 interface and 144 meV close to a TiO_2 interface, while the bulk value of 231 meV is recovered close to a parylene gate insulator.

For a given disorder potential in the organic semiconductor, localization effects roughly scale with the reciprocal bandwidth. Consequently, important bandwidth reductions enhance all localization effects and consequently decrease the mobility. It is important to note that in the present work the existence of a lattice polaron in the bulk of pentacene was considered as unlikely. Intramolecular vibrations are too fast to produce a polaron in a perfect pentacene crystal and their effect has been studied in Appendix C. Intermolecular phonons and librations with energies $\hbar\omega$ of the order of 10 meV are not coupled enough to the carrier to produce a well-defined lattice polaron, with a renormalized transfer integral of the order of 50 meV originating from the initial calculation of Cheng et al. [7]. However, when the transfer integral experiences a further reduction close to the gate interface as shown in Fig. 1, then the intrinsic lattice polaron can be excited, as suggested in a recent work [16]. A calculation is in progress to clarify this point. Moreover, an interface is rarely perfect from a structural point of view, and the fact that, due to significant internal field present at the interface, the carrier is constrained to probe more closely all the interface disorder,

enhancing the localization effects. Even "perfect" interfaces can be "intrinsic" sources of localization. In general, the electric dipole lattice induced by a charge carrier in the organic semiconductor is incommensurate with the dipole lattice induced in the gate material. In a perfect structure, the incommensurability of the electronic potential can open gaps in the semiconductor density of states. When the gate dielectric is not a single-crystal but a disordered structure, the same effect creates an electronic disorder which can be one of the sources of localization.

The effective bandwidth enters the mobility law but does not define it entirely. In disordered polymer channels, Veres et al. [5] have established a link between the effective width of the Gaussian distribution of electronic states and the mobility of the carrier which jumps from state to state according to the Gaussian Disorder Model [17]. In more ordered systems such as single-crystalline rubrene OFETs, a theoretical work is in progress to establish a quantitative link between the transfer integral and the mobility. It will elucidate the role of thermal, low-energy phonons which are, on the one side, sources of localization and on the other the key to the adiabatic diffusion of the carriers in the channel.

Acknowledgments

The authors acknowledge the financial support of the Swiss Federal Science Foundation under contract number 200020-105156.

APPENDIX A: ELECTRONIC POLARON AT THE INTERFACE

The electronic polarization of a molecular crystal, *i.e.* the formation of induced dipoles \mathbf{d} on the neutral molecules of the crystal in the field of an extra-charge, occurs on a time scale of $\tau \sim 10^{-15} - 10^{-16}$ s ($\hbar/\tau \sim 2$ eV). This is much faster than the carrier lifetime on a molecule which is typically $\tau_J \sim \hbar/J \sim 4 \times 10^{-14}$ s with $J \simeq 100$ meV, allowing one to treat the carrier as stationary on a molecular site during the polarization process.

1. Bulk

With the above approximation, we have calculated the polarization energy of a point-charge in bulk pentacene crystal to be $E_p \simeq -1.5$ eV [11] using the method of self-consistent polarization field to the dipolar approximation [8]. The pentacene crystal structure and parameters are given in Tab.I. The molecules involved in the discrete calculation are assumed to be inside a spherical cluster of radius R . The polarization energy varies linearly with the inverse radius of the cluster. The polarizabilities of the molecules along the (L, M, N) -directions were adjusted so that the polarization energy at large R matches the continuum limit $(1 - \epsilon_{\text{eff}}^{-1}) e^2 / 4\pi\epsilon_0 R$, where ϵ_{eff} is the effective dielectric constant in an anisotropic structure [18]. The convergence is fast and the calculated polarization energies for anthracene, $E_p \simeq -1.26$ eV, and pentacene, $E_p \simeq -1.5$ eV, are in good agreement with recently reported values [19].

As the charge carrier moves from one molecule to another, the polarization energy changes. In fact, when the electronic polarization energy and the induced-dipole distribution vary from site n to site $n + h$ due to different local crystal environment, the carrier will encounter a resistance to its motion. This leads to a renormalization of the bare transfer integral J . We introduced the parameter S_0 [11] as a way of describing quantitatively the polarizability effect on the transfer integral, *i.e.* $J^I = J \exp(-S_0)$. The quantity S_0 is closely related to the relative amplitudes and directions of the induced dipoles and is given through the relations [11],

$$S_0(h) = \frac{1}{2} \sum_i \sum_{l=1}^3 (X_{i,l}(n) - X_{i,l}(n+h))^2 \quad (\text{A1})$$

$$X_{i,l} = \frac{d_{i,l}}{2\sqrt{\epsilon\alpha_{ll}}} \quad (\text{A2})$$

where α_{ll} are the components of the polarizability, and ϵ , of the order of one electron-volt, is the energy difference between the ground state and the first-excited state of the neutral molecule [11]. The sites considered here, n and $n + h$, are the next-nearest neighbor along the crystal direction $\mathbf{d}_2 = -\frac{1}{2}\mathbf{a} + \frac{1}{2}\mathbf{b}$.

2. Interface

We now extend the above calculation to the case of charge carrier near the interface of pentacene with the dielectric insulator. In this case, the polarization cloud extends partly into the semiconductor and partly into the dielectric. For simplicity, we modelled the dielectric insulator as a cubic lattice. The Clausius-Mosotti relation is then applied to obtain the electronic polarizability of the molecules of the dielectric assuming a given high frequency permittivity,

$$\frac{\epsilon_{\infty,2} - 1}{\epsilon_{\infty,2} + 2} = \frac{1}{3\epsilon_0} N \alpha_e \quad (\text{A3})$$

$$N = \frac{\rho}{M} N_A \quad (\text{A4})$$

Here M and ρ are the molar mass and the density of the dielectric and N_A is the Avogadro number. The summation in Eq.A1 is then extended to include the induced dipoles in the semiconductor and the dielectric. For reasons of symmetry, the molecules involved in the discrete calculations are taken inside a cylindrical cluster on both sides of the interface. Beyond the cluster approximation, a continuum contribution is added to the polarization energy using standard electrostatics [20]. The polarization energy as a function of the distance from the interface is shown in Fig.2 for both the discrete and the continuous limits.

APPENDIX B: SQUEEZING OF THE CHARGE DISTRIBUTION AT THE INTERFACE

The self-trapping interfacial polarization electric field (see Appendix A) and the applied gate-field localize the excess charge on the pentacene molecule by pulling and squeezing the wavefunction towards or away from the interface depending on the relative magnitudes of the dielectric constants of pentacene and the gate-insulator. To get the average position and the spatial extent of the wavefunction of the excess charge, we used a model in which the pentacene molecule is considered as a pair of conjugated chains of eleven sites, each separated by a distance l that we treat in the tight-binding approximation. The basis wavefunction on each site, ψ_n , with $n = 1, \dots, 11$ satisfies the following set of equations,

$$E_0 \psi_n = -t_{//} (\psi_{n+1} + \psi_{n-1}) - nlqF \psi_n - V(nl) \psi_n \quad (\text{B1})$$

with the boundary conditions $\psi_0 = \psi_{12} = 0$ imposed at the two ends of the pentacene molecule. Here V is the image force potential, F is the applied gate-field, and $t_{//}$ is the intramolecular transfer integral. Upon solving this system of equations, we obtain the ground-state wavefunction as,

$$|\Psi_0\rangle = \sum_{i=1}^{11} \psi_n |n\rangle, \quad (\text{B2})$$

The spatial dependence of the average position of the excess charge on the chain will be given by,

$$\langle n \rangle = \sum_{n=1}^{11} n |\psi_n|^2 \quad (\text{B3})$$

Since the pentacene molecule is nearly perpendicular to the interface, the presence of interfacial fields localizes the charge at the extremity of the molecule. This has the effect of changing the thickness of the channel and, as a consequence, the bandwidth for charge propagation. Indeed, the transfer integral in acene crystals increases with the number of aromatic rings from naphthalene to pentacene [7, 21]. This can be related to the spatial extent of the excess charge on the acene molecule. The charge extent σ_n is defined as the width containing 80% of the charge density. We have chosen as in Appendix A the direction of higher transfer integral which determines the bandwidth. Therefore, the variation of the charge extension under the effect of the image force and the gate-field, will induce a corresponding change in the transfer integral of the pentacene molecules as shown in Fig. 3. For the calculation of the excess charge extension in the above model, the intramolecular transfer integral $t_{//}$ was set to 1eV. The values of the gate and image force fields are those found in Appendix A. However, a semi-empirical quantum chemistry calculation published recently [13] has shown that, probably due to exchange interactions between the carrier and the π -electrons in the pentacene molecule, the extra-charge distribution is not pulled and squeezed in the direction of the interface field by the extent predicted by the above model. Thus in the final result of Fig. 1 this effect has not been included. Figure 3 shows what would the final result be in the case where the squeezing calculated above in this appendix would indeed be effective.

APPENDIX C: BAND NARROWING DUE TO INTRAMOLECULAR VIBRATIONS

We now refer to the strong coupling of the extra charge to the intramolecular vibrations at 1360 cm^{-1} in pentacene. The coupling constant has been determined in acenes both experimentally and theoretically in Ref. [22]. The calculation of the band narrowing due to phonons has been presented by several authors [9, 10]. Here, we present a simplified version for dispersionless intramolecular vibrations.

The electron-phonon Hamiltonian of interest is written as,

$$H = \sum_{n,h} -J^{II} a_{n+h}^+ a_n + \sum_n \hbar\omega_0 b_n^+ b_n - \sqrt{E_B/\hbar\omega_0} (b_n^+ + b_n) a_n^+ a_n \quad (\text{C1})$$

where n represents the molecular sites; a_n^+ , a_n , b_n^+ , and b_n are the electron and phonon operators respectively. $g = \sqrt{E_B/\hbar\omega_0}$ is the usual coupling parameter. Since the phonon frequency $\hbar\omega_0$ is larger than the transfer integral J^{II} , we look for a variational solution of the Hamiltonian. The trial wavefunction is of the form,

$$|\psi_n\rangle = \sum_n u_n |n\rangle \otimes |\chi_n\rangle \quad (\text{C2})$$

where

$$|\chi_n\rangle = \exp(X_n^* b_n - X_n b_n^+) |0\rangle \quad (\text{C3})$$

describes the intramolecular vibrations of the molecule n on which the charge is located. The variational parameter X_n is determined by minimizing the energy

$$E = \langle \psi | H | \psi \rangle \quad (\text{C4})$$

Then

$$\begin{aligned} E = & - \sum_{n,h} J^{II} \exp\left(\frac{-|X_n|^2 + |X_{n+h}|^2}{2}\right) u_{n+h}^+ u_n \\ & - \sqrt{E_B/\hbar\omega_0} (X_n + X_n^*) |u_n|^2 + \sum_n \hbar\omega_0 |X_n|^2 \end{aligned} \quad (\text{C5})$$

We find $X_n = \sqrt{E_B/\hbar\omega_0}$ and the corresponding transfer integral,

$$J^{III} = J^{II} \exp(-E_B/\hbar\omega_0) \quad (\text{C6})$$

When thermal phonons are taken into account the thermal average value of the energy yields a temperature correction factor in the transfer integral given by,

$$J^{III} = J^{II} \exp \left(-\frac{E_B}{\hbar\omega_0} \coth \left(\frac{\hbar\omega_0}{2k_B T} \right) \right) \quad (C7)$$

In the present case, the temperature effect is completely negligible and the electron-phonon binding energy is just $-E_B$ per molecular site.

Taking the values in bulk pentacene from Ref. [22] with $E_B = 45$ meV, we obtain $J^{III} = 0.75J^{II}$. Close to the interface the band narrowing due to intramolecular vibrations is rather insensitive to the interfacial field. This is related to the fact that the phonon frequency and coupling constants are approximately the same in the acene series [22].

APPENDIX D: THE FRÖHLICH SURFACE POLARON

When a charge carrier is generated by the field effect at the interface between a molecular semiconductor and a gate insulator, it interacts with the surface phonons of the dielectric. This effect has been studied in Ref. [12] for an isotropic 3D molecular crystal in the adiabatic limit. Here, we consider this interaction in the case of a pentacene crystal where the carrier motion is essentially two-dimensional and for moderate electron-phonon coupling. Indeed, the residence time in a monolayer $\tau \sim \hbar/J_{\perp}$, with $J_{\perp} \sim 5$ meV is much larger than the time to polarize the dielectric given by $2\pi/\omega_s$, where $\hbar\omega_s = 46$ meV in Al_2O_3 [14]. However, the phonon frequency $\hbar\omega_s$ is of the same order of magnitude as the effective in-plane transfer integral $J^{III} \sim 60$ meV. The frequency ω_s is given by the following formula:

$$\omega_s^2 = \frac{1}{2} (\omega_L^2 + \omega_T^2), \quad (D1)$$

where ω_L and ω_T are the frequencies of the bulk longitudinal and transverse phonons. [23] The values of ω_s for the different dielectrics are reported in Tab. II

The electron-phonon interaction involving a charge in a particular monolayer of the crystal at a distance $z > 0$ from the interface is given by [8],

$$H_{\text{e-ph}} = \sum_q \frac{e}{\sqrt{q}} \sqrt{\frac{\pi \hbar \omega_s}{S \epsilon^*}} \sum_n e^{-qz} e^{i\mathbf{q} \cdot \mathbf{n}a} (b_q + b_{-q}^+) |\psi_n|^2 \quad (D2)$$

where $|\psi_n|^2$ is the charge density at site $\mathbf{n}a = (n_x a, n_y a)$. Here b_q and b_{-q}^+ are the annihilation and creation operators of the surface phonons in the gate material, ω_s their frequency, and S the surface area of the interface.

If $\epsilon_1(\omega)$ is the dielectric susceptibility of the molecular crystal, $\epsilon_{\infty,2}$ and $\epsilon_{0,2}$ the high and low frequency limits of the dielectric permittivity, the coupling constant $1/\epsilon^*$ is given by,

$$\frac{1}{\epsilon^*} = \frac{\epsilon_1 - \epsilon_{\infty,2}}{\epsilon_1(\epsilon_1 + \epsilon_{\infty,2})} - \frac{\epsilon_1 - \epsilon_{0,2}}{\epsilon_1(\epsilon_1 + \epsilon_{0,2})} \quad (\text{D3})$$

and the total Hamiltonian becomes,

$$H = -J^{III} a^2 \frac{p^2}{\hbar^2} + \sum_q \hbar \omega_s b_q^+ b_q + H_{\text{e-ph}} \quad (\text{D4})$$

where \mathbf{p} is the momentum of the charge carrier. Following Ref. [24], we introduce the total momentum of the system which is a constant of motion of the total Hamiltonian,

$$\mathbf{P} = \sum_q \hbar \mathbf{q} b_q^+ b_q + \mathbf{p} \quad (\text{D5})$$

We can transform the total Hamiltonian H to H' through the unitary transformation \hat{S} , so that H' no longer contains the charge coordinates,

$$H' = \hat{S}^{-1} H \hat{S} \quad (\text{D6})$$

with,

$$\hat{S} = \exp \left[i \left(\mathbf{P} - \sum_q b_q^+ b_q \mathbf{q} \right) \cdot \mathbf{n} a \right] \quad (\text{D7})$$

We obtain thus,

$$\begin{aligned} H' = & \sum_q \hbar \omega_s b_q^+ b_q + \sum_q V_q(z) (b_q + b_{-q}^+) \left[\mathbf{P}/\hbar - \sum_q b_q^+ b_q \mathbf{q} \right] J^{III} a \\ & + \left[\mathbf{P}/\hbar - \sum_q b_q^+ b_q \right] J^{III} a^2 \end{aligned} \quad (\text{D8})$$

where

$$V_q(z) = \frac{e}{\sqrt{q}} \sqrt{\frac{\pi \hbar \omega_s}{S \epsilon^*}} e^{-qz} \quad (\text{D9})$$

With the phonon frequency $\hbar \omega_s$ comparable to the effective transfer integral J^{III} , the adiabatic approximation is not applicable. However, the dimensionless parameter α_{eff} which describes the strength of the electron-phonon coupling decreases with the distance z to the interface as

$$\alpha_{\text{eff}} = \frac{e^2}{8\pi\epsilon_0\epsilon^*a} \frac{\exp(-2\pi z/a)}{\sqrt{\hbar \omega_s J^{III}}} \equiv \alpha e^{-2\pi z/a} \quad (\text{D10})$$

In our case, α_{eff} is of the order of 1 for a charge carrier located in the first monolayer. Then, we use a variational method to describe the interaction of the dressed charge carrier with the dielectric phonons [24]. Introducing a second unitary transformation,

$$\hat{U} = \exp \left(\sum_q b_q^+ f_q - b_q f_q^* \right) \quad (\text{D11})$$

where f_q will be chosen to minimize the energy

$$\begin{aligned} E = & \frac{\mathbf{P}^2}{\hbar} a^2 J^{III} + \sum_q (V_q f_q + V_q^* f_q^*) + J^{III} \left(\sum_q |f_q|^2 q^2 a^2 \right)^2 \\ & + \sum_q |f_q|^2 \left[\hbar \omega_s + J^{III} \left(q^2 a^2 - 2\mathbf{q} \cdot \frac{\mathbf{P}}{\hbar} a^2 \right) \right] \end{aligned} \quad (\text{D12})$$

We then find,

$$f_q = -\frac{V_q^*}{\hbar \omega_s + J^{III}} \left[q^2 a^2 - 2\frac{\mathbf{q} \cdot \mathbf{P}}{\hbar} a^2 (1 - \eta) \right] \quad (\text{D13})$$

where η satisfies the implicit equation

$$\eta \mathbf{P} = \frac{\sum_q |V_q|^2 \hbar \mathbf{q}}{\hbar \omega_s + J^{III} [q^2 a^2 - 2\frac{\mathbf{q} \cdot \mathbf{P}}{\hbar} a^2 (1 - \eta)]} \quad (\text{D14})$$

The carrier binding energy is obtained as $E_b = -\alpha I_1(z) \hbar \omega_s$ and the effective mass is $m^*/m = J^{III}/J^{IV} = 1 + 2\alpha I_2(z)$. As long as $J^{III} P^2 a^2 / \hbar^2$ is small ($\lesssim \hbar \omega_s$), we may obtain $E(P^2)$ to first order in an expansion in powers of $\left(\frac{J^{III} P^2 a^2}{\hbar \omega_s \hbar^2} \right)$. On doing so, one readily gets

$$E = -\alpha I_1(z) \hbar \omega_s + \frac{P^2 a^2}{\hbar^2} \frac{J^{III}}{[1 + 2\alpha I_2(z)]} \quad (\text{D15})$$

where

$$I_1(z) = \int_0^{\pi \sqrt{J^{III}/\hbar \omega_s}} \frac{dy}{1+y^2} \exp \left(-\frac{2z}{a} \sqrt{\frac{\hbar \omega_s}{J^{III}}} y \right) g(y) \quad (\text{D16})$$

and

$$I_2(z) = \int_0^{\pi \sqrt{J^{III}/\hbar \omega_s}} \frac{y^2 dy}{(1+y^2)^3} \exp \left(-\frac{2z}{a} \sqrt{\frac{\hbar \omega_s}{J^{III}}} y \right) g(y) \quad (\text{D17})$$

Here the term given by

$$g(y) = \frac{\sinh \left[y \sqrt{\frac{\hbar \omega_s}{J^{III}}} \frac{\ell}{a} \right]}{y \sqrt{\frac{\hbar \omega_s}{J^{III}}} \frac{\ell}{a}} \quad (\text{D18})$$

- [1] V. Podzorov, E. Menard, A. Borissov, V. Kiryukhin, J. A. Rogers, and M. E. Gershenson, *Phy. Rev. Lett.* **93**, 086602 (2004).
- [2] F. Dinelli, M. Murgia, P. Levy, M. Cavalleni, F. Biscarini, and D. M. de Leeuw, *Phys. Rev. Lett.* **92**, 116802 (2004).
- [3] J. H. Kang, D. A. da Silva Filho, J. L. Bredas, and X.-Y. Zhu, *Appl. Phys. Lett.* **86**, 152115 (2005).
- [4] M. Daraktchiev, A. von Mühlén, F. Nüesch, M. Schaer, M. Brinkmann, M. N. Bussac, and L. Zuppiroli, *New Journal of Physics* **7**, 133 (2005).
- [5] J. Veres, S. D. Ogier, S. W. Leeming, D. C. Cupertino, and S. M. Khaffaf, *Adv. Func. Mater.* **13**, 199 (2003).
- [6] A. F. Stassen, R. W. I. de Boer, N. N. Iosad, and A. F. Morpurgo, *Appl. Phys. Lett.* **85**, 3899 (2004).
- [7] Y. C. Cheng, R. J. Silbey, D. A. da Silva Filho, J. P. Calbert, J. Cornil, J. L. Bredas, *J. Chem. Phys.* **118**, 3764 (2003).
- [8] E. A. Silinsh and V. Čápek, *Organic Molecular Crystals* (AIP Press, New York, 1994).
- [9] J. Appel, *Solid Stat. Phys.* **25**, 193 (1968).
- [10] A. S. Davydov, *Théorie du Solide* (Edition Mir, 1980).
- [11] M. N. Bussac, J. D. Picon, and L. Zuppiroli, *Europhys. Lett.* **66**, 392 (2004).
- [12] N. Kirova, and M. N. Bussac, *Phys. Rev. B* **68**, 235312 (2003).
- [13] J. C. Sancho-García, G. Horowitz, J. L. Brédas, and J. Cornil, *J. Chem. Phys.* **119**, 12563 (2003).
- [14] M. Schubert, T. E. Tiwald, and C. M. Herzinger, *Phys. Rev. B* **61**, 8187 (2000).
- [15] D. A. da Silva Filho, E. G. Kim, and J. L. Brédas, *Adv. Mater.* **17**, 1072 (2005).
- [16] K. Hannewald, and P. A. Bobbert, *Phys. Rev. B* **69**, 075212 (2004); K. Hannewald, V. M. Stojanović, J. M. Schellekens, P. A. Bobbert, G. Kresse, and J. Hafner, *ibid.* **69**, 075211 (2004).
- [17] H. Bässler, *Phys. Stat. Sol. B* **175**, 11 (1993).
- [18] P. J. Bounds, and R. W. Munn, *Chem. Phys.* **44**, 103 (1979).

- [19] E. V. Tsiper, and Z. G. Soos, Phys. Rev. B **68**, 085301 (2003).
- [20] J. D. Jackson, Classical Electrodynamics (Wiley & Sons, New York, 1999), p. 154.
- [21] J. L. Bredas, J. P. Calbert, D. A. da Silva Filho, and J. Cornil, Proc. Natl. Acad. Sci. **99**, 5804 (2002).
- [22] V. Coropceanu, M. Malagoli, D. A. da Silva Filho, N. E. Gruhn, T. G. Bill, and J. L. Bredas, Phys. Rev. Lett. **89**, 275503 (2002).
- [23] J. Sak, Phys. Rev. D **6**, 3981 (1972).
- [24] T. D. Lee, F. E. Low, and D. Pines, Phys. Rev. **90**, 297 (1953).

Figure 1: The largest transfer integral for charge propagation in pentacene close to the interface with the gate insulator as a function of the relative static permittivity of the dielectric. The charge carrier is located on the first monolayer close to the interface. The high frequency dielectric constant $\epsilon_{\infty,2}$ for the gate insulators is: 2.65 for parylene C; 2.37 for SiO₂; 3.1 for Al₂O₃; 4.12 for Ta₂O₅; and 6.5 for TiO₂.

Figure 2: The image potential $E_p(z)$ at the interface is given in the continuous approximation and in our lattice model. At large distances from the interface the electronic polarization energy in the bulk is recovered.

Figure 3: These are the same results as in Fig. 1 but calculated with another set of data as explained in Appendix B. The largest transfer integral for charge propagation in pentacene close to the interface with the gate insulator is plotted as a function of the relative static permittivity of the dielectric. The charge-carrier is assumed to be located on the first monolayer. The inset depicts the case where the charge-carrier is on the second monolayer. These curves cumulate all the effects calculated in this work. In contrast to the results of Fig. 1 we have assumed here that the carrier distribution is pulled away or squeezed towards the interface according to the calculation in Appendix B. This effect is enhanced with respect to the semi-empirical model of Ref. [13]. Here the effective mass depends even on the gate field. At present, the corresponding values calculated in Fig. 1 are considered more reliable.

Table 1: Crystal constants of pentacene [R. B. Campbell et al., Acta Cryst. **14**, 705 (1961)].

Table 2: Values of the surface phonon frequencies used in the calculations of Appendix D together with the coupling constant α (see text).

Table 3: Reduction factors of the transfer integral through the steps discussed in the text. Cases of bulk pentacene and interfaces with vacuum and different dielectric oxides are shown along with the time scales characterizing each process. Here the second effect which is related to charge displacement on the molecule was excluded (see text).

Crystal constants (\AA)	a	b	c
	7.9	6.06	16.01
Crystal constants (deg)	α	β	γ
	101.9	112.6	85.8
Dielectric constant ^a	L	M	N
	5.336	3.211	2.413

^aE.V. Tsiper and Z.G. Soos, Phys. Rev. B **68**, 085301 (2003).

TABLE I:

	ω_s (cm^{-1})	α
SiO ₂ ^a	480	2.84
Al ₂ O ₃ ^b	386	5.24
Ta ₂ O ₅ ^c	390	6.17
TiO ₂ ^d	280	4.84

^aJ. Humlíček, A. Röseler, Thin Solid Films **234**, 332 (1993)

^bM. Schubert, et al., Phys. Rev. B **61**, 8187 (2000)

^cE. Franke, et al., J. Appl. Phys. **88**, 5166 (2000)

^dR. Sikora, J. Phys. Chem. Solids **66**, 1069 (2005)

TABLE II:

	Molecular polarization	Intramolecular charge vibration	Surface phonons	final result
Typical time scales	$\sim 10^{-15}$ s	$\sim 2 \times 10^{-14}$ s	$\sim 8 \times 10^{-14}$ s	
Reduction factors	J^I/J	J^{III}/J^I	J^{IV}/J^{III}	J^{IV}/J
Pentacene bulk	0.79	0.75	1	0.593
Pentacene/vacuum	0.76	0.75	1	0.57
Pentacene/SiO ₂	0.77	0.75	0.815	0.47
Pentacene/Al ₂ O ₃	0.77	0.75	0.69	0.398
Pentacene/Ta ₂ O ₅	0.77	0.75	0.65	0.375
Pentacene/TiO ₂	0.77	0.75	0.64	0.37

TABLE III:

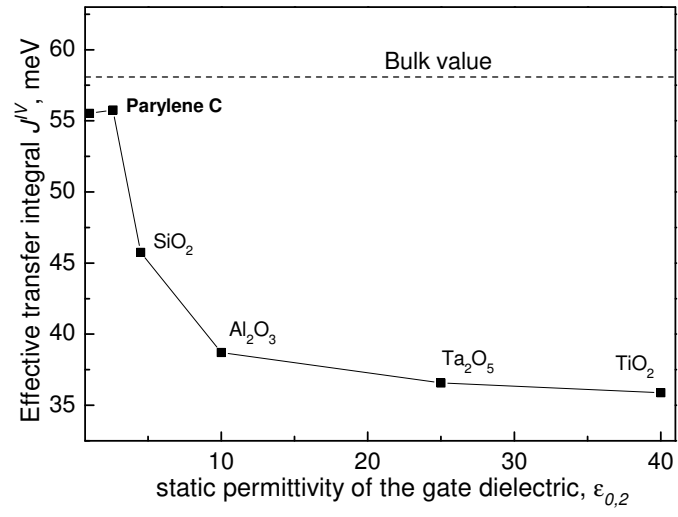


FIG. 1:

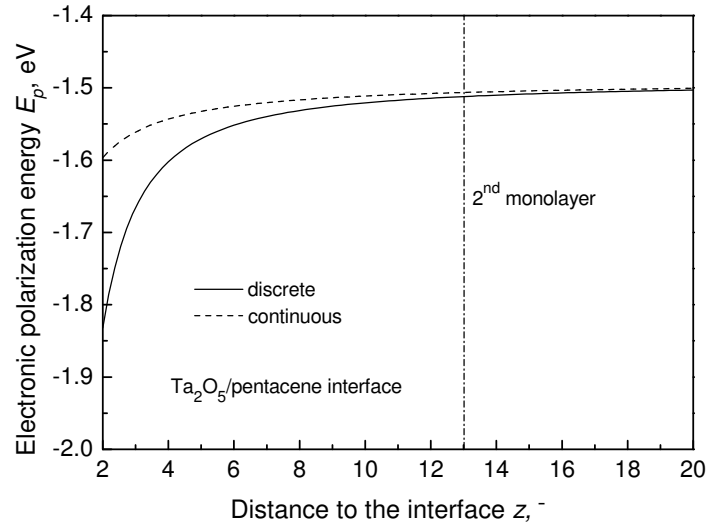


FIG. 2:

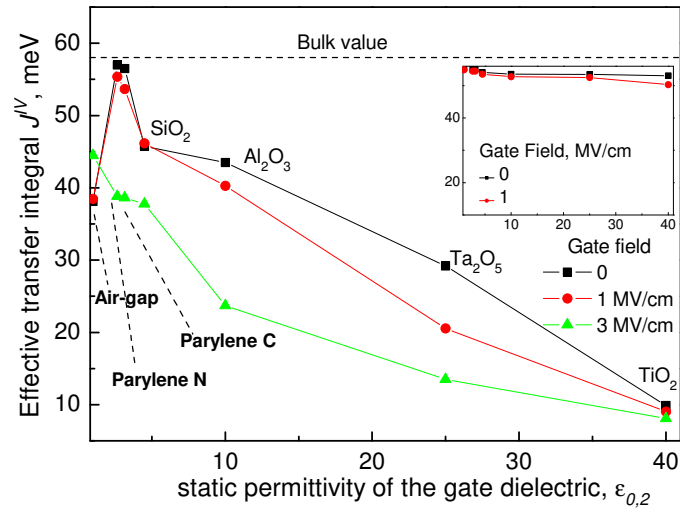


FIG. 3: